# Neuroligin-3 in Dopamine Neurons Promotes Behavioral and Neurobiological Adaptations to Chronic Morphine Exposure

**Abbreviated title**: Neuroligin-3 Regulates Responses to Morphine

Dieter D. Brandner[1,2], Cassandra L. Retzlaff[3], Bethany J. Stieve[1], Paul G. Mermelstein[3], & Patrick E. Rothwell[3,*]

[1]Graduate Program in Neuroscience, University of Minnesota, Minneapolis, MN, 55455

[2]Medical Scientist Training Program, University of Minnesota, Minneapolis, MN, 55455

[3]Department of Neuroscience, University of Minnesota, Minneapolis, MN, 55455

*Corresponding Author:

Patrick E. Rothwell, Ph.D.
4-142 Wallin Medical Biosciences Building
2101 6th Street SE
Minneapolis, MN, 55455
Phone: 612-626-8744
Email: rothwell@umn.edu

Number of pages: 30
Number of figures: 6
Number of tables: 1

Number of words for abstract: 239 (out of 250 maximum)
Number of words for introduction: 561 (out of 650 maximum)
Number of words for discussion: 1,265 (out of 1,500 maximum)

**Conflict of interest statement**: The authors declare no competing financial interests.

**Acknowledgements**: Research reported in this publication was supported by the University of Minnesota's MnDRIVE (Minnesota's Discovery, Research, and Innovation Economy) initiative, as well as National Institutes of Health grants F30 DA007234 (DDB), T32 DA052109 (PGM, DDB), R00 DA037279 (PER), and R01 DA048946 (PER). The University of Minnesota MnDRIVE Optogenetics Core provided technical support for fiber photometry experiments. Some of the viral vectors used in this study were generated by the University of Minnesota Viral Vector and Cloning Core. We thank Adrina Kocharian and Marc Pisansky for technical assistance, as well as Emilia Lefevre, Mohammed Mashal, Joshua Melander, Robert Meisel, Bailey Remmers, Carlee Toddes, and Brian Trieu for stimulating discussions.

## ABSTRACT

Chronic opioid exposure causes structural and functional changes in brain circuits, which may contribute to opioid use disorders. Synaptic cell-adhesion molecules are prime candidates for mediating this opioid-evoked plasticity. Neuroligin-3 (NL3) is a postsynaptic adhesion protein that shapes synaptic function at multiple sites in the mesolimbic dopamine system. We therefore studied how genetic knockout of NL3 alters responses to chronic morphine in male mice. Constitutive NL3 knockout caused a persistent reduction in psychomotor sensitization after chronic morphine exposure, as well as a change in the topography of locomotor stimulation produced by morphine. This latter change was recapitulated by conditional genetic deletion of NL3 from cells expressing the Drd1 dopamine receptor, whereas the reduction in psychomotor sensitization was recapitulated by conditional genetic deletion from dopamine neurons. In the absence of NL3 expression, dopamine neurons in the ventral tegmental area showed diminished activation following chronic morphine exposure, as measured by *in vivo* calcium imaging with fiber photometry. This altered pattern of dopamine neuron activity may be driven by aberrant forms of opioid-evoked synaptic plasticity in the absence of NL3: dopamine neurons lacking NL3 showed weaker synaptic inhibition at baseline, which was subsequently strengthened after chronic morphine. In total, our study highlights neurobiological adaptations in dopamine neurons of the ventral tegmental area that correspond with increased behavioral sensitivity to opioids, and further suggests that NL3 expression by dopamine neurons provides a molecular substrate for opioid-evoked adaptations in brain function and behavior.

## SIGNIFICANCE STATEMENT

Exposure to opioids and other drugs of abuse can cause long-lasting changes in the brain. Some of the most durable alterations involve functional and structural changes at synapses in brain reward circuits, including dopamine neurons in the ventral tegmental area and their projection to the nucleus accumbens. Synaptic cell-adhesion molecules support structural and functional aspects of synaptic transmission. Dysregulation of these molecules has been implicated in addiction and other neuropsychiatric disorders. We find that a specific synaptic cell-adhesion molecule, neuroligin-3, mediates changes in brain reward circuits caused by morphine exposure. In the absence of neuroligin-3, male mice are less sensitive to the behavioral effects of chronic morphine exposure, and dopamine neurons in the ventral tegmental area do not function normally.

## INTRODUCTION

Drugs of abuse target the mesolimbic dopamine projection, with a final common pharmacologic effect of increased extracellular dopamine levels in the nucleus accumbens (NAc) (Di Chiara and Imperato, 1988). Morphine and other opioids specifically increase the firing rate of dopamine neurons in the ventral tegmental area (VTA) by activating mu opioid receptors expressed on inhibitory synaptic inputs (Johnson and North, 1992; Matsui et al., 2014), thus enhancing dopamine release by a disinhibitory mechanism. Chronic opioid exposure produces a variety of neurobiological adaptations in mesolimbic circuitry, including functional and structural changes at synaptic connections in both the VTA and NAc (Hearing et al., 2018; Doyle and Mazei-Robison, 2021). These adaptations may contribute to the development of opioid use disorders, but the molecular basis of these adaptations remains poorly understood.

Synaptic cell adhesion molecules play a critical role in sculpting synaptic structure and function (Siddiqui and Craig, 2011; Sudhof, 2017), and thus represent potential molecular mediators of drug-evoked plasticity (Giza et al., 2013; Muskiewicz et al., 2018). This includes the neurexin and neuroligin families of adhesion molecules, which have been genetically linked to substance use disorders and other neuropsychiatric conditions (Jamain et al., 2003; Hishimoto et al., 2007; Lachman et al., 2007; Sanders et al., 2011; Docampo et al., 2012). Neuroligin-3 (NL3) is a particularly intriguing candidate for mediating drug-evoked plasticity within the mesolimbic dopamine system, since it has functional roles in both VTA dopamine neurons and NAc medium spiny projection neurons (MSNs). Genetic knockout of NL3 alters the subunit composition of AMPA receptors in VTA dopamine neurons (Bariselli et al., 2018) and causes synaptic disinhibition of D1-MSNs in the NAc (Rothwell et al., 2014). Similar forms of synaptic dysfunction have been reported after chronic exposure to drugs of abuse (Carlezon et al., 1997; Bellone and Luscher, 2006; Kim et al., 2011; Koo et al., 2014), suggesting genetic knockout of NL3 may alter behavioral and neurobiological responses to addictive substances like morphine.

To explore the potential role of NL3 in neurobehavioral adaptations caused by chronic morphine exposure, we studied the impact of constitutive genetic knockout of NL3, as well as conditional genetic knockout from specific cell types within mesolimbic circuits. We find that constitutive NL3 knockout males exhibit a change in spatial organization of locomotor activity following morphine exposure, which we refer to as locomotor topography (Mickley et al., 1990), as well as a persistent attenuation of psychomotor sensitization following chronic morphine exposure (Shuster et al., 1975). Conditional genetic knockout revealed a double-dissociation

in the cell types where NL3 deletion produced these effects: NL3 deletion from D1-MSNs altered locomotor topography after morphine exposure, whereas NL3 deletion from dopamine neurons persistently attenuated psychomotor sensitization following chronic morphine.

Psychomotor sensitization is one behavioral manifestation of the enhanced sensitivity of the mesolimbic dopamine system that develops after intermittent opioid exposure (Robinson and Berridge, 1993), and is initiated by opioid receptor activation in the VTA (Vezina et al., 1987; Radke et al., 2011). We therefore explored morphine-evoked neurobiological adaptations in dopamine neurons. In the absence of NL3 expression, VTA dopamine neurons showed an attenuation of activity after chronic morphine exposure, as well as altered inhibitory synaptic input. Together, these results indicate that NL3 has multiple distinct functions integral to the behavioral opioid response at discrete loci in the mesolimbic dopamine system. The function of NL3 in VTA dopamine neurons appears to be particularly critical for regulating the manner in which these cells adapt to chronic morphine exposure, as well as for long-lasting enhancement of behavioral sensitivity to opioids.

## MATERIALS AND METHODS

### Subjects

Mice were housed in groups of 2-5 per cage, on a 12-hour light cycle (0600h – 1800h) at ~23° C with food and water provided ad libitum. Experimental procedures were conducted between 1000h – 1600h, were approved by the Institutional Animal Care and Use Committee of the University of Minnesota, and conformed to the National Institutes of Health *Guidelines for the Care and Use of Laboratory Animals*. All mouse lines were maintained on a C57Bl/6J genetic background. Constitutive NL3 knockout animals (The Jackson Laboratory Strain #008394) were generated as previously described (Tabuchi et al., 2007). Conditional NL3 knockout animals were generated as previously described (Rothwell et al., 2014), with loxP sites flanking exons 2 and 3 of the *Nlgn3* gene. Floxed NL3 mice were crossed with Drd1-Cre BAC transgenic FK150 (Gong et al., 2007), Adora2a-Cre BAC transgenic KG139 (Gerfen et al., 2013), or DAT-IRES-Cre knock-in (Backman et al., 2006). These Cre driver lines were used to conditionally knockout NL3 in D1-MSNs, D2-MSNs, or dopamine neurons, respectively. Due to X-linkage of the *Nlgn3* gene, all experiments described in this study were conducted using

male mice, because it was possible to generate wild-type and knockout littermates from a single breeding scheme, and thus control for parental genotype.

**Gene Expression**

Quantitative RT-PCR was performed on tissue punches containing the dorsal and ventral striatum, as previously described (Lefevre et al., 2020; Toddes et al., 2021). Tissue was snap frozen on dry ice and stored at -80°C. RNA was extracted and isolated using the RNeasy Mini Kit (Qiagen) according to manufacturer instructions. A NanoDrop One microvolume spectrophotometer (Thermo Fisher Scientific, Waltham, MA) was used to measure RNA concentration and verify that samples had A260/A280 purity ratio ≥ 2. Reverse transcription was performed using Superscript III (Invitrogen, Eugene, OR). For each sample, duplicate cDNA reactions and subsequent qPCR reactions were conducted in tandem on both samples. Mouse β-actin mRNA was used as the endogenous control, with primer detection sequences of 5'—GAC GGC CAG GTC ATC ACA T—3' and 5'—CCA CCG ATC CAC ACA GAG TA—3'. Primer sequences for detection of NL3 were forward 5'—CAC TGT CTC GGA TTG CTT CA—3' and reverse 5'—TTC CCA GGG CAA TAC AGT CTC—3'. Quantitative RT-PCR using SYBR green (BioRad, Hercules, CA) was carried out with a Lightcycler 480 II (Roche, Basel, Switzerland) using the following cycle parameters: 1 x (30 sec @ 95°C), 35 x (5 sec @ 95°C followed by 30 sec @ 60°C). Results were analyzed by comparing the C(t) values of the treatments tested using the ΔΔC(t) method. Expression values of target genes were first normalized to the expression value of β-actin. The mean of cDNA replicate reactions was used to quantify the relative target gene expression.

**Behavioral Responses to Morphine Administration**

Morphine hydrochloride (Mallinckrodt) was dissolved in sterile 0.9% saline and delivered subcutaneously (5 mL/kg) by bolus injection at one of several doses (2, 6.32, or 20 mg/kg). We have previously used this series of doses to measure the acute psychomotor response to morphine (Toddes et al., 2021), as well as long-lasting psychomotor sensitization (Lefevre et al., 2020). The day prior to the first acute morphine injection, animals were habituated to the behavior apparatus and given an equivalent volume of 0.9% saline subcutaneously. This was followed by exposure to increasing morphine doses of 2, 6.32, and 20 mg/kg morphine on consecutive days.

Thermal antinociception was tested in a plexiglass cylinder on a 55°C hot plate (IITC Life Scientific), 15 minutes after morphine administration and just prior to placing animals in open-field chambers (Lefevre et al., 2020). Percent maximum possible antinociceptive effect (%MPE) was calculated as the percentage difference between the measured nociceptive response latency following morphine administration and baseline nociceptive response latency following saline administration divided by the difference between the maximum response latency and baseline response latency. Nociceptive responses included jumping, hind paw shaking, and hind paw licking. Maximum response latency was defined as 30 sec; animals that failed to respond after 30 sec were removed for the apparatus to avoid tissue damage.

We tested open-field locomotor activity for 60 minutes in a clear plexiglass arena (ENV-510, Med Associates) contained within a sound-attenuating chamber. Psychomotor sensitization consisted of seven consecutive doses of daily morphine administered subcutaneously at 20 mg/kg. To minimize the contextual effects of the behavior apparatus on psychomotor sensitization, open field locomotion was only measured during saline habituation and following morphine administration on Day 1 and Day 7. Morphine challenge injections were delivered 21 days following the final day of morphine sensitization and were conducted in a manner analogous to acute dose-response.

**Viral Vectors and Stereotaxic Surgery**

The plasmid encoding syn-Flex-jGCaMP8m (Addgene plasmid #162378) was a gift from GENIE Project (Zhang et al., 2021), and packaged in AAV9 by the University of Minnesota Viral Vector and Cloning Core. The plasmid pAAV-EF1a-DIO-eYFP (Addgene viral prep #27056-AAV9) was a gift from Karl Deisseroth. Intracranial virus injection and optical fiber implantation were performed as previously described (Pisansky et al., 2019). Briefly, mice were anesthetized with a ketamine-xylazine cocktail (100:10 mg/kg), and a burr hole was drilled above target coordinates for the ventral tegmental area (AP -2.9, ML +0.04; DV -4.5). A 33-gauge Hamilton syringe containing the viral solution was lowered to these target coordinates using a stereotaxic apparatus (David Kopf Instruments, Los Angeles, CA). A volume of 500nL of virus was injected at a rate of 100 nL/min. A 6 mm long, 400 µm diameter fiber-optic cannula with 0.48 NA (Doric Lenses: MFC_400/430-0.48_6.0mm_MF2.5_FLT) was inserted just above the site of viral injection (+0.01 mm DV), before being fixed in place with dual-cure resin (Patterson Dental, Inc.) and anchored in place with two skull screws inserted into the parietal bone.

**Fiber Photometry**

Continuous fiber photometry recordings were conducted in open-top chambers for 15 minutes prior to and 30 minutes following morphine injection on Days 1 and 7. Real-time data were acquired using a RZ5P fiber photometry workstation (Tucker Davis Technologies). As previously described (Pisansky et al., 2019), 470 nm and 405 nm LEDs (ThorLabs) were modulated at distinct carrier frequencies (531 Hz and 211 Hz, respectively), and passed through a fluorescence mini cube (Doric Lenses) coupled into a patch cord (400 µm, 0.48 NA). The distal end of the patch cord was connected to the implanted fiberoptic cannula by a fitted ceramic sleeve. Fluorescence was projected back through the mini cube and focused onto a photoreceiver (Newport Model 2151). Signals were sampled at 6.1 kHz, demodulated in real-time, and saved for offline analysis. The change in fluorescent signal (ΔF/F) was calculated within each session as described (Lerner et al., 2015). Each channel was low-passed filtered (<2Hz) and a linear least-squared model fit the isosbestic control signal (405 nm) to the calcium-dependent signal (470 nm). Change in fluorescence was calculated as ([470nm signal – fitted 405nm signal]/[fitted 405nm signal]). Data was smoothed by calculating the mean ΔF/F over a sliding window of 50 sec along the entire duration of the normalized ΔF/F recording, to reveal slow fluctuations in GCaMP fluorescence caused by morphine exposure. The average fluorescent signal for 200 sec prior to morphine injection and 1000 sec following morphine injection was computed to determine the pre-morphine baseline and post-morphine ΔF/F. The difference between these two averages was calculated as an index of VTA dopamine neuron activity in response to morphine administration. After the end of repeated morphine administration, the D2 agonist apomorphine (5 mg/kg, s.c.) was administered on Day 8. Recordings were analyzed as indicated above to compute the average ΔF/F fluorescence before and after injection. All animals exhibited a precipitous drop in ΔF/F immediately following administration of apomorphine, due to activation of somatodendritic D2 autoreceptors on VTA dopamine neurons (Lacey et al., 1987).

**Immunohistochemistry**

To confirm virus expression and optic cannula placement, all mice were deeply anaesthetized using a phenytoin/pentobarbitol mixture (Beuthanasia, 200 mg/kg, i.p.), then transcardially perfused with ice-cold 0.1% PBS followed by ice-cold 4% paraformaldehyde in 0.1% PBS. Brains were fixed overnight in 4% paraformaldehyde in 0.1% PBS then sliced at 50 µm thickness using a vibratome (Leica VT1000S). Free-floating

coronal sections containing the nucleus accumbens were incubated for 3 hours in blocking solution containing 0.2% Triton-X, 2% normal horse serum, and 0.05% Tween20. Sections were then incubated for 48 hours with primary antibodies (Invitrogen mouse anti-eGFP 1:1000, Cat. # A-11120), washed three times, and incubated overnight with secondary antibodies (Abcam goat anti-mouse Alexa Fluor 488 IgG 1:1000, Cat. # ab150117). Slides were washed and mounted using ProLong Gold Antifade mountant with DAPI (Life Technologies). Stained tissue sections were imaged on a laser-scanning confocal microscope (model TCS SPE, Leica Microsystems).

**Electrophysiology**

$NL3^{fl/y}$;$DAT^{Cre/wt}$ and $NL3^{wt/y}$;$DAT^{Cre/wt}$ animals that received stereotaxic injection of AAV9-EF1a-DIO-eYFP (see above) were allowed to recover 5-14 days before the start of drug treatment. All mice were habituated to injection and then treated with either morphine (20 mg/kg, s.c.) or saline for seven consecutive days. Twenty-four hours after the final injection, mice were deeply anesthetized with isoflurane and perfused with ice cold sucrose solution containing (in mM): 228 sucrose, 26 NaHCO3, 11 glucose, 2.5 KCl, 1 NaH2PO4-H2O, 7 MgSO4-7H20, 0.5 CaCl2-2H2O. Brains were then rapidly dissected and placed in cold sucrose for slicing. Horizontal hemisected slices (225 µm) containing the VTA were collected using a vibratome (Leica VT1000S) and allowed to recover in a warm (33°C) holding chamber with artificial cerebrospinal fluid (aCSF) containing (in mM): 119 NaCl, 26.2 NaHCO3, 2.5 KCl, 1 NaH2PO4-H2O, 11 glucose, 1.3 MgSO4-7H2O, 2.5 CaCl2-2H2O. Slices recovered for 10-15 min and then equilibrated to room temperature for at least one hour before use. Slices were transferred to a submerged recording chamber and continuously perfused with aCSF at a rate of 2 mL/min at room temperature. All solutions were continuously oxygenated (95% O2/5% CO2).

Dopamine neurons in the VTA were identified by viral expression of eYFP using an Olympus BX51W1 microscope. Whole-cell voltage-clamp recordings were made with borosilicate glass electrodes (3-5 MΩ) filled with (in mM): 125 CsCl, 10 TEA-Cl, 10 HEPES, 0.1 EGTA, 3.3 QX-314 ($Cl^-$ salt), 1.8 MgCl2, 4 Na2-ATP, 0.3 Na-GTP, 8 Na2-phosphocreatine (pH 7.3 adjusted with CsOH; 276 mOsm). All recordings were performed using a MultiClamp 700B amplifier (Molecular Devices), filtered at 2 kHz, and digitized at 10 kHz. Data acquisition and analysis were performed online using Axograph software. Series resistance was monitored continuously, and experiments were discarded if resistance changed by >20%. To pharmacologically isolate spontaneous inhibitory postsynaptic currents, the extracellular bath solution contained the AMPA receptor antagonist NBQX (10 uM)

and the NMDA receptor antagonist D-APV (50 uM). These were inward currents at a holding potential of -60 mV, due to the high chloride concentration in the internal pipette solution. At least 200 events per cell analyzed was acquired across 15 sec sweeps, filtered at 0.5 kHz, and detected using an amplitude threshold of 5.5-6.5 pA and a signal-to-noise ratio threshold of 2.5 standard deviations.

### Experimental Design and Statistical Analyses

Constitutive NL3 knockout mice (Figure 1) were generated by breeding heterozygous females ($NL3^{-/+}$) with wild-type males ($NL3^{+/y}$). Conditional NL3 knockout mice were generated by crossing $NL3^{fl/fl}$ dams with sires that were Drd1-Cre hemizygotes (Figure 2), Adora2a-Cre hemizygotes (Figure 3), or $DAT^{Cre/wt}$ heterozygotes (Figure 4). For fiber photometry experiments (Figure 5) and slice physiology experiments (Figure 6), homozygous $DAT^{Cre/Cre}$ sires were crossed with heterozygous $NL3^{fl/+}$ dams, so that all offspring were $DAT^{Cre/wt}$ heterozygotes with or without a floxed NL3 allele. These breeding schemes generated male offspring with either intact or complete loss of NL3 expression, but female offspring with only partial loss of NL3 expression, so we focused our analysis on male mice in this manuscript. For clarity, the details regarding each of these breeding schemes are repeated at the beginning of each section describing the corresponding results.

Sample sizes are indicated in figure legends as well as graphs that display individual data points, along with measures of central tendency (mean) and variability (SEM). Data were analyzed in factorial ANOVA models using GraphPad Prism 9 and IBM SPSS Statistics v24, with repeated measures on within-subject factors or mixed-effect models to handle missing data. For main effects or interactions involving repeated measures, the Greenhouse-Geisser correction was applied to control for potential violations of the sphericity assumption. This correction reduces the degrees of freedom, resulting in non-integer values. Significant interactions were decomposed by analyzing simple effects (i.e., the effect of one variable at each level of the other variable). Significant main effects were analyzed using LSD post-hoc tests. The Type I error rate was set to $\alpha=0.05$ (two-tailed) for all comparisons

## RESULTS

### NL3 knockout mice exhibit less psychomotor sensitization after chronic morphine exposure

To study the effects of genetically deleting NL3 from all synapses in the brain (Figure 1A), we utilized a constitutive NL3 knockout mouse line (Tabuchi et al., 2007). Since the gene that encodes NL3 is located on the

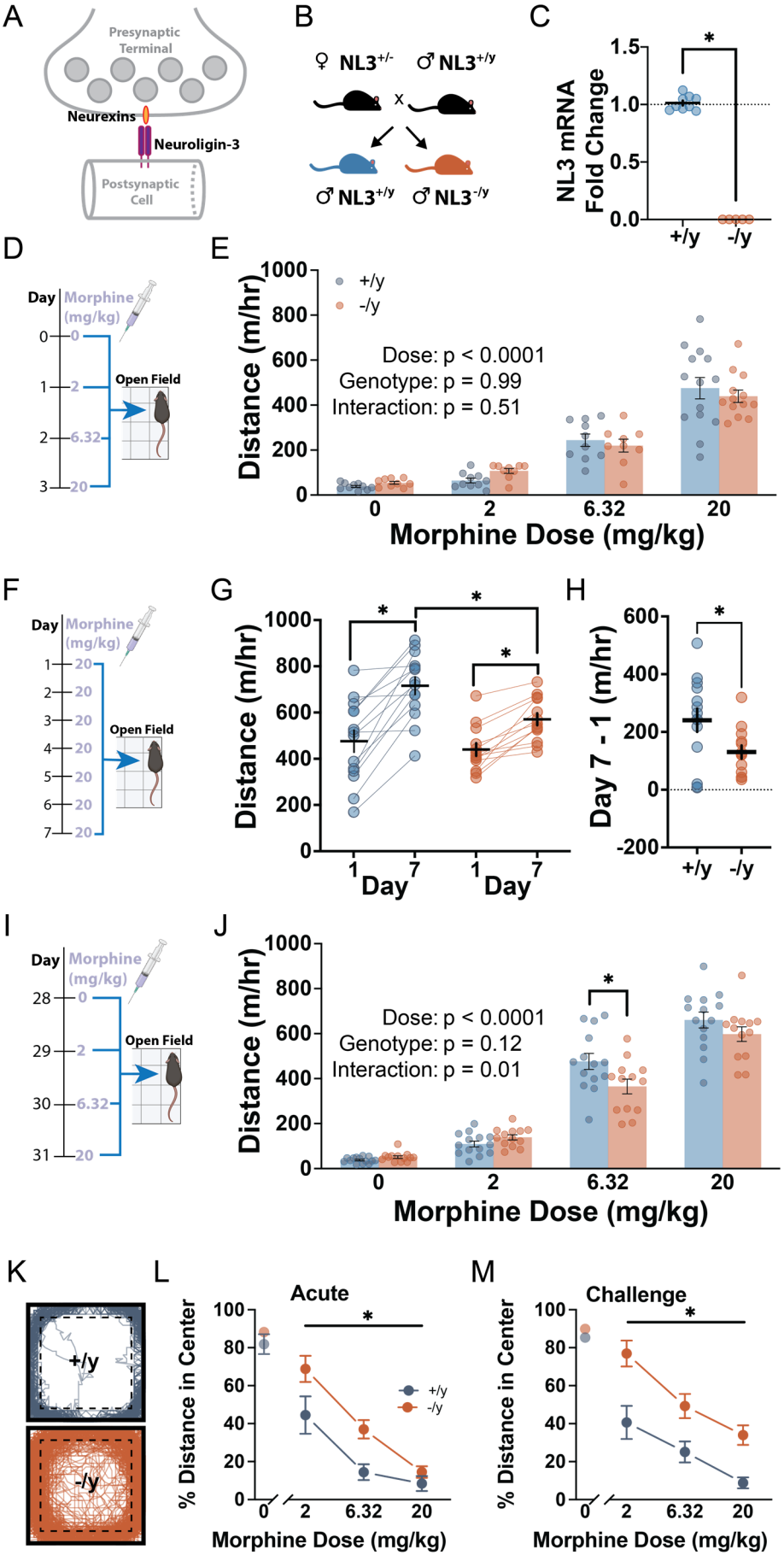


**Figure 1. Responses to acute and chronic morphine exposure in NL3 constitutive knockout mice.** **(A)** Cartoon showing synaptic localization of NL3. **(B)** Breeding scheme. **(C)** Quantification of NL3 mRNA in striatal tissue using quantitative RT-PCR in +/y (n=9) and -/y (n=5) littermates. **(D)** Schematic showing dose sequence for acute morphine exposure. **(E)** Distance travelled following each acute injection in +/y (n=10) and -/y (n=9) littermates at 0-6.32 mg/kg, and +/y (n= 14) and -/y (n=13) littermates at 20 mg/kg, along with statistical results from factorial ANOVA analysis. **(F)** Schematic showing chronic morphine exposure with locomotor activity tested on Days 1 and 7. **(G)** Distance travelled following morphine exposure on Days 1 and 7 in +/y (n=14) and -/y (n=13) littermates. **(H)** Difference in locomotion on Days 1 and 7 in the same cohort of animals. **(I)** Schematic showing dose sequence for morphine challenge. **(J)** Distance travelled following each challenge injection of morphine, along with statistical results from factorial ANOVA analysis. **(K)** Track plots illustrating path of travel after challenge with 6.32 mg/kg morphine. **(L, M)** Percentage of total distance traveled in the central area after acute (**L**) or chronic (**M**) morphine exposure, in the same groups shown above. *p<0.05 comparing groups with simple effect tests **(G)**, unpaired t-test **(H),** Fisher's LSD *post-hoc* test **(J)**, or main effect in ANOVA **(L, M)**.

X-chromosome, we generated male NL3 hemizygous knockouts ($NL3^{-/y}$) and wild-type littermates ($NL3^{+/y}$) by breeding heterozygous females ($NL3^{-/+}$) with wild-type males ($NL3^{+/y}$) (Figure 1B). Genetic knockout was validated using pooled bilateral tissue punches from the dorsal striatum and nucleus accumbens (Figure 1C), which demonstrated robust depletion of NL3 mRNA in knockout mice ($t_{12} = 35.70$, $p<0.0001$). We first examined behavioral response to acute morphine exposure by injecting increasing doses of morphine (2-20 mg/kg, s.c.) prior to a test of open field activity (Figure 1D). All mice exhibited a dose-dependent increase in locomotor activity (Figure 1E), as indicated by a main effect of Dose ($F_{1.45,36.87} = 90.23$, $p<0.0001$). However, there was no main effect of Genotype ($F_{1,76} < 1$) or interaction ($F_{3,76} < 1$), indicating that distance traveled was similar in both genotypes after acute morphine exposure.

We next measured behavioral responses following seven daily injections of 20 mg/kg morphine (Figure 1F), a chronic pattern of exposure that causes psychomotor sensitization as well as analgesic tolerance (Lefevre et al., 2020). Open field activity was measured after injection on Days 1 and 7 (Figure 1G), to monitor the development of psychomotor sensitization. As expected, distance traveled increased substantially after chronic morphine administration, as indicated by a main effect of Day ($F_{1,25} = 61.79$, $p<0.0001$). There was also a significant Day x Genotype interaction ($F_{1,25} = 5.40$, $p=0.029$), indicating a significant reduction in distance travelled by $NL3^{-/y}$ mutants versus $NL3^{+/y}$ controls on Day 7 ($p=0.014$), despite similar distance traveled on Day 1. This result was most apparent after computing the change in distance traveled between Day 1 and Day 7 for each individual animal (Figure 1H), revealing a significant reduction in psychomotor sensitization in $NL3^{-/y}$ mutants ($t_{25}=2.32$, $p = 0.029$). Notably, the antinociceptive effect of acute morphine exposure and development of antinociceptive tolerance were similar in $NL3^{-/y}$ and $NL3^{+/y}$ mice (Table 1), indicating that NL3 plays a role in some but not all behavioral adaptations to chronic morphine exposure.

We have previously documented the durability of psychomotor sensitization after this regimen of chronic morphine exposure (Lefevre et al., 2020). We thus waited 21 days after the end of chronic exposure, and then challenged the same cohorts of animals with increasing doses of morphine (2-20 mg/kg) (Figure 1I). Analysis of distance travelled in the open field (Figure 1J) revealed a significant Dose $\times$ Genotype interaction ($F_{3,75} = 3.886$, $p=0.012$), a phenotype not observed after acute morphine exposure (Figure 1E). Distance travelled after a challenge injection of 6.32 mg/kg morphine was significantly reduced in $NL3^{-/y}$ mutants versus $NL3^{+/y}$ controls (p

= 0.030). These results suggest that neuroadaptations supporting psychomotor sensitization are dependent upon NL3 for complete and persistent expression.

**Table 1. Hot plate antinociception in NL3 constitutive knockout mice after acute and chronic morphine.**

| Genotype | Day 1 %MPE | Day 7 %MPE |
|---|---|---|
| $NL3^{+/y}$ (15) | 96.89 ± 2.31 | 50.57 ± 7.24 |
| $NL3^{-/y}$ (13) | 85.17 ± 6.42 | 41.05 ± 3.77 |
| *Statistical Results* | $t_{26} = 1.82$; $p = 0.081$ | $t_{26} = 1.11$; $p = 0.28$ |

All data are presented as mean +/- SEM; number in parenthesis represent sample sizes for each genotype.

**Altered locomotor topography after morphine exposure in NL3 knockout mice**

After morphine injection, the locomotor hyperactivity exhibited by wild-type mice leads to a path of travel along the perimeter of the activity chamber (Mickley et al., 1990). In contrast, $NL3^{-/y}$ mutants exhibited a more curvilinear path of travel after morphine injection, bypassing the corners of the chamber and instead traveling through more central areas (Figure 1K). We quantified the topography of locomotor activity by calculating the percentage of total distance traveled through the interior of the chamber. There were no significant differences between genotypes in this measure prior to acute morphine exposure (Figure 1L) ($t_{14} = 1.13$, $p = 0.28$) or morphine challenge (Figure 1M) ($t_{22} = 1.98$, $p = 0.06$). There was a main effect of Dose after both acute morphine exposure ($F_{1.47,20.63} = 46.67$, $p < 0.001$) and morphine challenge ($F_{1.69,35.57} = 35.59$, $p < 0.001$), indicating that higher doses of morphine caused a greater shift in the distribution of locomotor activity to the perimeter of the activity chamber. There was also a main effect of Genotype after both acute morphine exposure ($F_{1,14} = 7.81$, $p = 0.014$) and morphine challenge ($F_{1,21} = 18.78$, $p < 0.001$), supporting the conclusion that $NL3^{-/y}$ mutants have a greater percentage of distance travelled through the interior of the chamber. This change in locomotor topography was evident after both acute and chronic morphine exposure, whereas distance travelled by $NL3^{-/y}$ mutants was only different after chronic morphine exposure, providing initial evidence that these two phenotypes may be dissociable.

**Conditional NL3 deletion from D1-MSNs alters locomotor topography but not sensitization after morphine exposure**

We next sought to determine if behavioral responses to morphine are regulated by conditional NL3 deletion from specific cell types within the mesolimbic dopamine system. Prior work has shown that NL3 is expressed at a particularly high level by D1-MSNs in the NAc, and conditional genetic deletion from this specific cell type recapitulates some behavioral phenotypes of constitutive NL3 knockout mice (Rothwell et al., 2014). Synaptic inhibition of D1-MSNs is diminished in the absence of NL3 expression (Rothwell et al., 2014), and this D1-MSN disinhibition may drive rotational patterns of movement (Engeln et al., 2021), such as the curvilinear path of travel exhibited by NL3 knockout mice after morphine exposure. D1-MSNs are also a critical site for structural and functional plasticity underlying persistent psychomotor sensitization (Dobi et al., 2011; Pascoli et al., 2011; Hearing et al., 2016), suggesting NL3 in these cells could be necessary for the full expression of morphine sensitization.

We began by crossing $NL3^{fl/fl}$ dams with sires from a BAC transgenic line expressing Cre-recombinase under the transcriptional control of the Drd1 dopamine receptor (Gong et al., 2007), to achieve selective conditional knockout of NL3 from D1-MSNs (Figure 2A) as previously described (Rothwell et al., 2014). After acute morphine exposure (Figure 2B), all mice exhibited a dose-dependent increase in locomotor activity, as indicated by a main effect of Dose ($F_{1.509,34.70} = 128.3$, $p<0.0001$). However, there was no main effect of Genotype ($F_{1,23} < 1$) or interaction ($F_{3,69} < 1$), indicating similar distance traveled in both genotypes after acute morphine exposure. Contrary to our expectation, $NL3^{fl/y}$;D1-Cre mice exhibited normal development of psychomotor sensitization after chronic morphine exposure (Figure 2C). Analysis of these data revealed a main effect of Day ($F_{1,23} = 90.47$, $p<0.0001$), but no main effect of Genotype ($F_{1,23} < 1$) or interaction ($F_{1,23} = 2.091$, $p = 0.16$). The similar degree of sensitization was also apparent in analysis of the change in distance traveled between Day 1 and Day 7 for each individual animal (Figure 2D). Both genotypes also showed a similar response to morphine challenge (Figure 2E), with a main effect of Dose ($F_{1.448,27.52} = 78.14$), but no main effect of Genotype ($F_{1,19} < 1$) or interaction ($F_{3,57} < 1$).

There were no significant differences between genotypes in locomotor topography prior to acute morphine exposure (Figure 2F) ($t_{24} < 1$) or morphine challenge (Figure 2G) ($t_{20} = 2.02$, $p = 0.057$). However, there was a Genotype x Dose interaction after morphine challenge ($F_{1.94,38.88} = 3.94$, $p = 0.029$), with

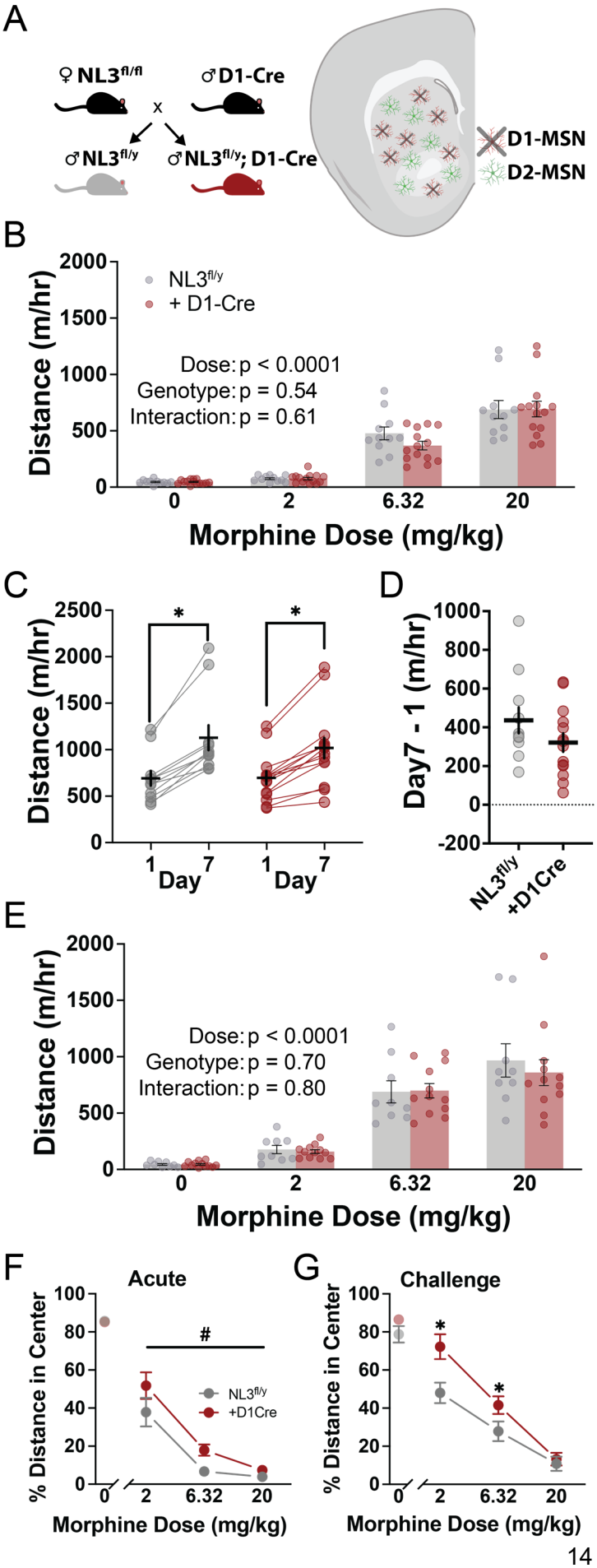


**Figure 2. Responses to acute and chronic morphine exposure after conditional NL3 knockout from D1-MSNs. (A)** Breeding scheme used to achieve conditional knockout of NL3 in D1-MSNs. **(B)** Distance travelled following each acute injection in NL3$^{fl/y}$, without (n=11) and with D1-Cre (n=14), along with statistical results from factorial ANOVA**. (C)** Distance travelled for the same cohorts following chronic morphine exposure on Days 1 and 7. **(D)** Difference in locomotion on Days 1 and 7. **(E)** Distance travelled following each challenge injection of morphine, along with statistical results from factorial ANOVA analysis. **(F, G)** Percentage of total distance traveled in the central area after acute (**F**) or chronic (**G**) morphine exposure, in the same groups shown above. *p<0.05 and #p<0.10 for simple effect of Day in each genotype **(C),** main effect in ANOVA **(F)**, or Fisher's LSD *post-hoc* test **(G)**.

significant differences between genotypes after challenge with 2 and 6.32 mg/kg morphine. After acute morphine, there was also a trend toward a main effect of Genotype that did not reach statistical significance ($F_{1,24}$ = 3.86, p = 0.061). $NL3^{fl/y}$;D1-Cre mice thus show a change in locomotor topography after morphine exposure, but no change in psychomotor sensitization, providing further evidence for a dissociation between these phenotypes.

**Conditional NL3 deletion from D2-MSNs does not affect behavioral responses to morphine**

Since conditional NL3 deletion from D1-MSNs did not recapitulate the attenuation of psychomotor sensitization seen in NL3 constitutive knockouts, we next considered the role of D2-MSNs, the other major neuron type within the NAc and striatum. Opioid exposure causes functional as well as structural changes in D2-MSNs (Graziane et al., 2016; Hearing et al., 2016), which could be mediated by NL3. As previously described (Rothwell et al., 2014), we crossed $NL3^{fl/fl}$ dams with sires from a BAC transgenic line expressing Cre-recombinase under the transcriptional control of the Adora2a adenosine receptor (A2a-Cre). This genetic strategy allowed us to target D2-MSNs (Figure 3A), which also exhibit enriched expression of Adora2a (Schiffmann and Vanderhaeghen, 1993), while avoiding other cell types that express Drd2 (Durieux et al., 2009).

After acute morphine exposure (Figure 3B), all mice exhibited a dose-dependent increase in locomotor activity, as indicated by a main effect of Dose ($F_{2.031,46.71}$ = 231.3, p<0.0001). However, there was no main effect of Genotype ($F_{1,23}$ < 1) or interaction ($F_{3,69}$ < 1), indicating that distance traveled was similar in both genotypes after acute morphine exposure. $NL3^{fl/y}$;A2a-Cre mice also exhibited normal development of psychomotor sensitization after chronic morphine exposure (Figure 3C). Analysis of these data revealed a main effect of Day ($F_{1,16}$ = 163.6, p<0.0001), but no main effect of Genotype ($F_{1,16}$ < 1) or interaction ($F_{1,16}$ = 3.743, p = 0.071), with a similar change in distance traveled between Day 1 and Day 7 (Figure 3D). Both genotypes also showed a similar response to morphine challenge (Figure 3E), with a main effect of Dose ($F_{2.167,49.83}$ = 224.4, p<0.0001), but no main effect of Genotype ($F_{1,23}$ < 1) or interaction ($F_{3,69}$ < 1). Finally, $NL3^{fl/y}$;A2a-Cre mice exhibited normal locomotor topography before and after both acute morphine exposure (Figure 3F) and morphine challenge (Figure 3G). These results are consistent with a lower level of NL3 expression by D2-MSNs (Rothwell et al., 2014), and suggest this neuronal population is not involved in the altered behavioral responses to morphine exhibited by NL3 constitutive knockout mice.

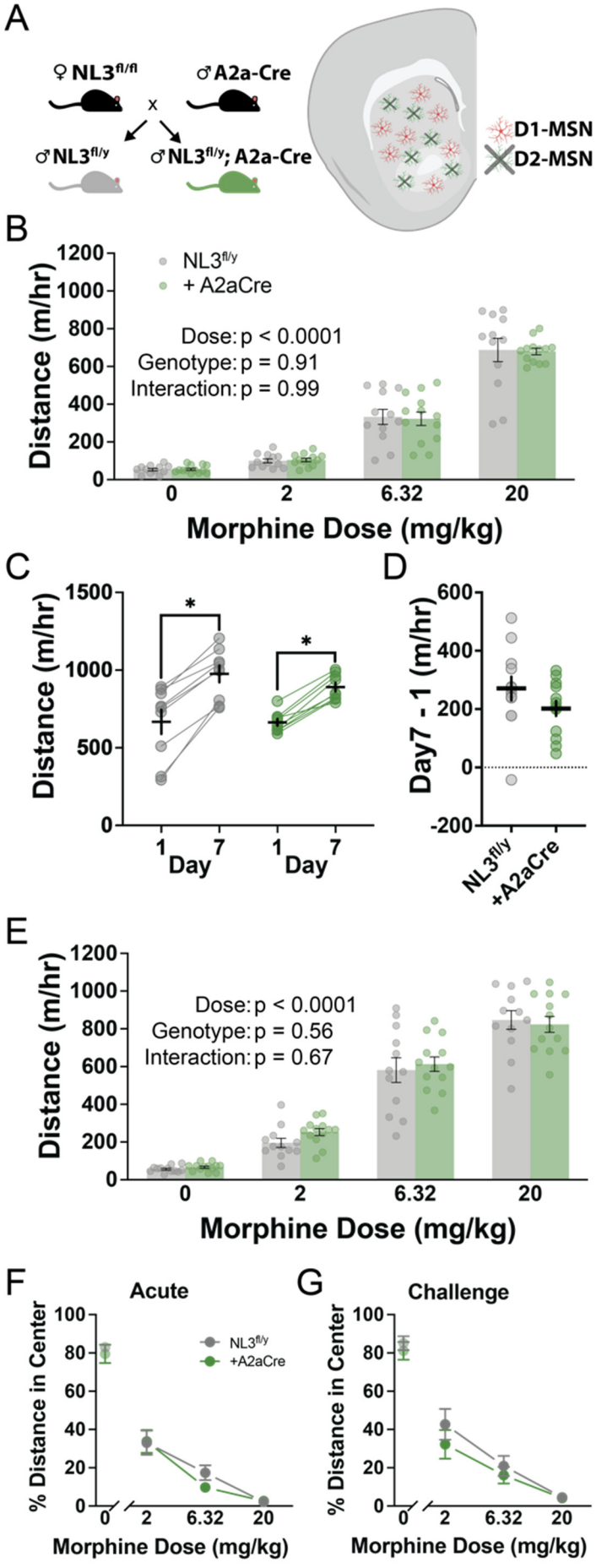


**Figure 3. Responses to acute and chronic morphine exposure after conditional NL3 knockout from D2-MSNs. (A)** Breeding scheme used to achieve conditional knockout of NL3 in D1-MSNs. **(B)** Distance travelled following each acute injection in NL3$^{fl/y}$, without (n=12) and with A2a-Cre (n=13), along with statistical results from factorial ANOVA**. (C)** Distance travelled for the same cohorts following chronic morphine exposure on Days 1 and 7. **(D)** Difference in locomotion on Days 1 and 7. **(E)** Distance travelled following each challenge injection of morphine, along with statistical results from factorial ANOVA analysis. **(F, G)** Percentage of total distance traveled in the central area after acute (**F**) or chronic (**G**) morphine exposure, in the same groups shown above. *p<0.05 for simple effect of Day in each genotype **(C).**

**Conditional NL3 deletion from dopamine neurons attenuates psychomotor sensitization without affecting locomotor topography**

Drug-evoked adaptations in the nucleus accumbens contribute to the long-lasting expression of psychomotor sensitization, but the induction of sensitization involves drug action in the VTA, which contains dopamine neurons that form the mesolimbic projection (Vezina et al., 1987; Vezina and Leyton, 2009; Radke et al., 2011). Previous studies have shown that NL3 depletion alters the physiology of dopamine neurons, and NL3 expression by these cells is required for normal social behavior (Bariselli et al., 2018; Hornberg et al., 2020). To achieve selective conditional knockout of NL3 from dopamine neurons (Figure 4A), we crossed $NL3^{fl/fl}$ dams with DAT-IRES-Cre ($DAT^{Cre/wt}$) sires (Backman et al., 2006). This genetic strategy allowed us to selectively target dopamine neurons while avoiding non-dopaminergic cells (Lammel et al., 2015).

After acute morphine exposure (Figure 4B), all mice exhibited a dose-dependent increase in locomotor activity, as indicated by a main effect of Dose ($F_{1.713,29.12} = 224.1$, $p<0.0001$). However, there was no main effect of Genotype ($F_{1,17} < 1$) or interaction ($F_{3,51} < 1$), indicating similar distance travelled in both genotypes after acute morphine exposure. After chronic morphine exposure (Figure 4C), there was a main effect of Day ($F_{1,17} = 152.1$, $p<0.0001$) as well as a significant Day x Genotype interaction ($F_{1,17} = 5.986$, $p = 0.026$). This interaction indicated an attenuation of sensitization in $NL3^{fl/y}$;$DAT^{Cre/wt}$ mice, which was apparent after computing the change in distance traveled between Day 1 and Day 7 for each individual animal ($t_{13} = 3.37$, $p = 0.0037$) (Figure 4D). This reduced magnitude of sensitization was also evident after morphine challenge (Figure 4E), with a main effect of Dose ($F_{1.730,68} =220.0$, $p<0.0001$) as well as a significant Dose $\times$ Genotype interaction ($F_{3,51} = 3.75$, $p=0.016$). Distance travelled after a challenge injection of 20 mg/kg morphine was significantly reduced in $NL3^{fl/y}$;$DAT^{Cre/wt}$ mutants versus $NL3^{fl/y}$ controls ($p = 0.032$). Conditional genetic deletion of NL3 from dopamine neurons thus recapitulated the diminished psychomotor sensitization seen after chronic morphine exposure in constitutive NL3 knockout mice. Finally, $NL3^{fl/y}$;$DAT^{Cre/wt}$ mutants mice exhibited a normal path of travel before and after both acute morphine exposure (Figure 4F) and morphine challenge (Figure 4G), demonstrating a double-dissociation in the neuronal populations where NL3 regulates psychomotor sensitization and locomotor topography after morphine exposure.

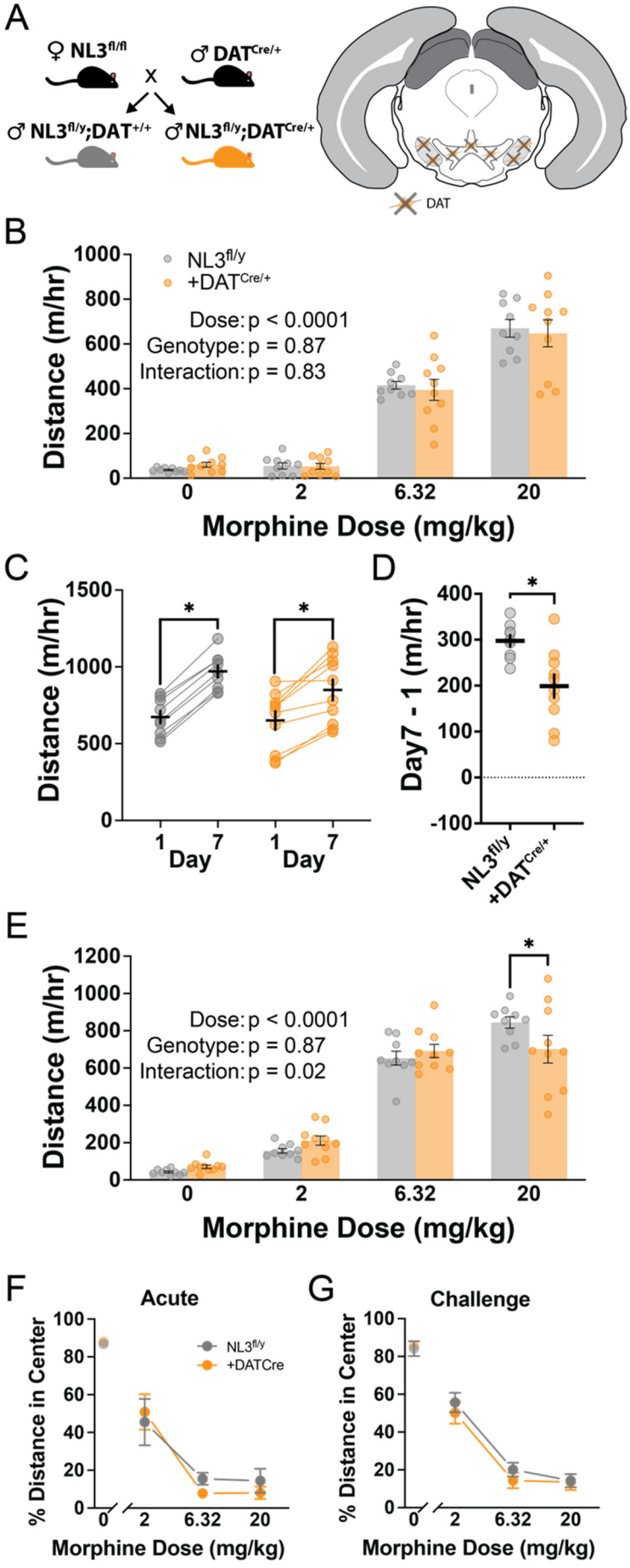


**Figure 4. Responses to acute and chronic morphine exposure after conditional NL3 knockout from dopamine neurons. (A)** Breeding scheme used to achieve conditional knockout of NL3 in dopamine neurons. **(B)** Distance travelled following each acute injection in NL3$^{fl/y}$, without (n=9) and with DAT-Cre (n=10), along with statistical results from factorial ANOVA**. (C)** Distance travelled for the same cohorts following chronic morphine exposure on Days 1 and 7. **(D)** Difference in locomotion on Days 1 and 7. **(E)** Distance travelled following each challenge injection of morphine, along with statistical results from factorial ANOVA analysis. **(F, G)** Percentage of total distance traveled in the central area after acute (**F**) or chronic (**G**) morphine exposure, in the same groups shown above. *p<0.05 for simple effect of Day in each genotype **(C),** unpaired t-test **(D),** or Fisher's LSD *post-hoc* test **(E)**.

**Photometric signature of morphine sensitization is absent in VTA dopamine neurons lacking NL3**

Opioid administration excites dopamine neurons through a disinhibitory mechanism, involving activation of opioid receptors on inhibitory synaptic inputs (Johnson and North, 1992; Matsui et al., 2014). The influence of opioid administration on dopamine neuron activity also changes over the course of chronic opioid exposure (Georges et al., 2006; Sun et al., 2014). This led us to ask whether NL3 expression shapes the response of dopamine neurons over the course of chronic morphine administration *in vivo*. We used calcium imaging with fiber photometry to conduct longitudinal measurements of dopamine neuron activity (Gunaydin et al., 2014; Corre et al., 2018). To compare these measurements in presence and absence of NL3 expression in dopamine neurons, we bred homozygous $DAT^{Cre/Cre}$ sires with heterozygous $NL3^{fl/+}$ dams, so that male offspring were $DAT^{Cre/wt}$ heterozygotes with or without a floxed NL3 allele ($NL3^{fl/y}$ or $NL3^{+/y}$) (Figure 5A). All mice received unilateral stereotaxic injection of an adeno-associated viral vector encoding Cre-dependent jGCaMP8m (AAV9-hSyn-Flex-jGCaMP8m) into the VTA, followed by implantation of an optical fiber just above the site of virus injection (Figure 5B). Post-mortem histological analysis confirmed robust expression of jGaMP8m in the midbrain (Figure 5C), with anatomical placement of fiber-optic implants in the VTA of both genotypes (Figure 5D).

To record the response of dopamine neurons to morphine administration, we delivered blue light (470 nm) to monitor calcium-dependent changes in jGCaMP8m fluorescence, as well as purple light (405 nm) as an isosbestic control to correct for bleaching and movement artifact (Figure 5E). At the end of each experiment, to confirm that the fluorescent signal correlated with the activity of dopamine neurons, we administered apomorphine (5 mg/kg) to activate D2-autoreceptors located on the somatodendritic compartment of VTA dopamine neurons (Lacey et al., 1987). As expected, we observed a consistent decrease in fluorescent signal following apomorphine administration in mice of both genotypes (Figure 5F).

We recorded GCaMP signal on Day 1 and 7 of morphine exposure to measure the response of VTA dopamine neurons (Figure 5G). On the intervening Day 2 and Day 6, we measured distance travelled in the open field after morphine administration (Figure 5H). We again observed a trend toward attenuation of sensitization in $NL3^{fl/y}$;$DAT^{Cre/wt}$ mice, which was apparent after computing the change in distance traveled for each individual animal ($t_{12}$ = 2.01, p = 0.067) (Figure 5I). Control animals showed a modest increase in ΔF/F following morphine administration on Day 1, which tended to increase after 7 days of morphine (example trace

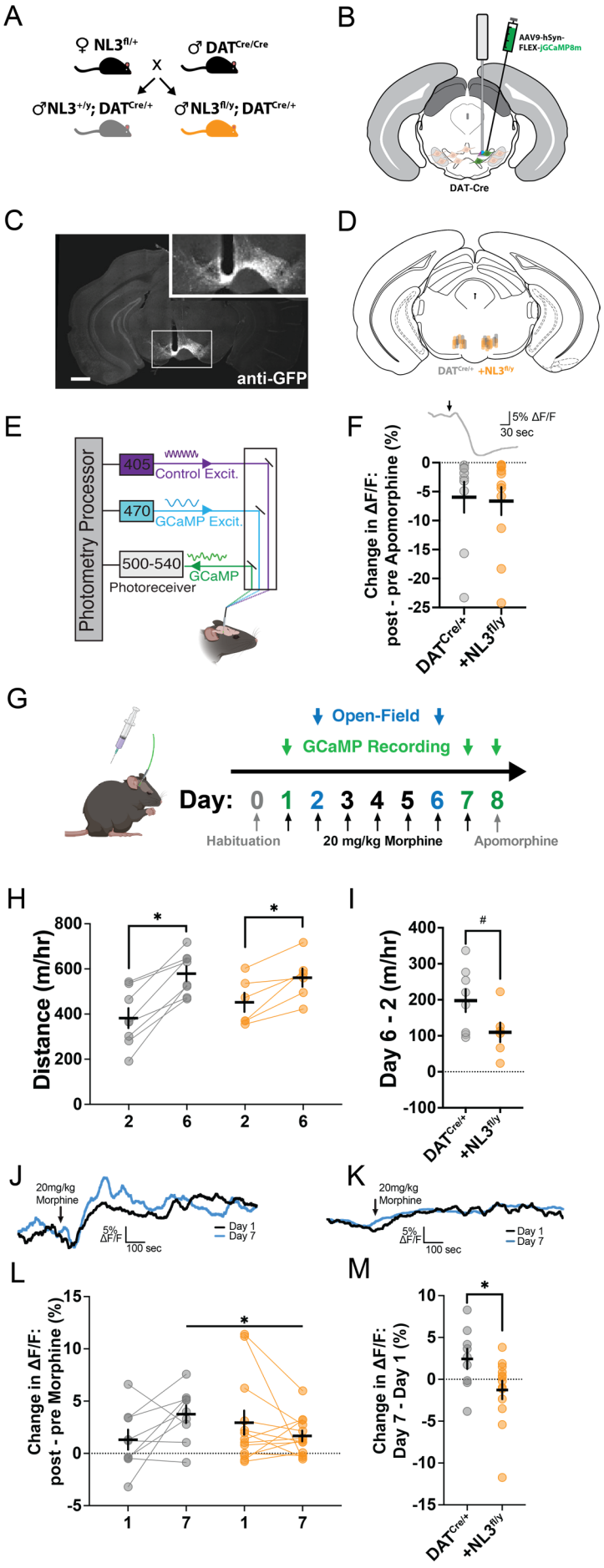


**Figure 5. Fiber photometry recordings from VTA dopamine neurons after chronic morphine exposure. (A)** Breeding scheme used to generate DAT-Cre mice with or without floxed NL3. **(B)** Cartoon showing unilateral stereotaxic injection of AAV9-hSyn-FLEX-jGCaMP8m into the VTA, with fiber optic implant placed just above the injection site. **(C)** Representative image of jGCaMP8m expression in the VTA (Scale bar = 500µm). **(D)** Anatomical locations of fiber optic implants in individual mice of each genotype. **(E)** Cartoon showing fiber photometry system. **(F)** Effect of apomorphine (5mg/kg, s.c.), injected at the time indicated by the arrow (top), on fluorescent signal in $DAT^{Cre/+}$ mice without (n=9) or with $NL3^{fl/y}$ (n=13). **(G)** Experimental timeline showing habituation (Day 0), 20 mg/kg morphine injections (Days 1-7), and apomorphine injection (Day 8). Photometry recordings were performed on Day 1 and Day 7, and locomotion was tested on Day 2 and Day 6. **(H)** Distance travelled following morphine exposure on Days 2 and 6, measured in a subset of $DAT^{Cre/+}$ mice without (n=8) or with $NL3^{fl/y}$ (n=6). **(I)** Difference in locomotion on Days 1 and 7. **(J, K)** Representative photometry traces from $DAT^{Cre/+}$ mice without **(J)** or with $NL3^{fl/y}$ **(K)**, on Day 1 and Day 7 of morphine exposure. **(L)** Difference in fluorescent signal before and after morphine injection on Day 1 and Day 7. **(M)** Change in difference score across days for individual mice. *p<0.05 or #p<0.10 for simple effect of Day in each genotype **(H),** unpaired t-test **(I, M),** or Fisher's LSD *post hoc* test **(L)**.

Figure 5J, quantified in Figure 5L), providing a putative photometric correlate of sensitization in VTA dopamine neurons. In contrast, although $NL3^{fl/y}$;$DAT^{Cre/wt}$ animals showed a robust increase in GCaMP fluorescence on Day 1, this signal did not increase with repeated morphine administration, and in fact was numerically lower on Day 7. This pattern was reflected in a significant Day x Genotype interaction ($F_{1,20} = 5.34$, $p = 0.032$), as well as a significant difference between genotypes in the change in fluorescent response to morphine across repeated exposure ($t_{20} = 2.24$, $p = 0.032$) (example trace Figure 5K, quantified in Figure 5M). This result suggests that loss of NL3 expression prevents dopamine neurons from becoming increasingly sensitive to repeated daily morphine treatment.

**VTA dopamine neurons lacking NL3 exhibit differential synaptic inhibition**

Opioid administration excites dopamine neurons by activating opioid receptors on inhibitory synaptic inputs (Johnson and North, 1992; Matsui et al., 2014), and NL3 mutations can alter the function of numerous inhibitory synapses in the brain (Tabuchi et al., 2007; Foldy et al., 2013; Rothwell et al., 2014). To assess inhibitory synaptic function in dopamine neurons, we again generated $DAT^{Cre/wt}$ mice with or without a floxed NL3 allele (Figure 5A). All mice received bilateral stereotaxic injection of an adeno-associated viral vector encoding Cre-dependent eYFP (AAV9-EF1a-DIO-eYFP) into the VTA (Figure 6A). This allowed us to identify dopamine neurons in acute brain slices based on yellow fluorescence and perform whole-cell patch-clamp recordings of spontaneous inhibitory postsynaptic currents (sIPSCs) in the presence of glutamate receptor antagonists (Figure 6B). Similar to previous experiments, these mice received seven daily injections of morphine (20 mg/kg) or saline, and acute brain slices were prepared 24 hours after the final injection (Figure 6C).

Analysis of sIPSC amplitude revealed a significant Genotype x Treatment interaction ($F_{1,16} = 6.94$, $p = 0.018$) (Figure 6D). In control groups receiving saline injections, sIPSC amplitude was decreased in $NL3^{fl/y}$ mice compared to $NL3^{+/y}$ littermates ($p = 0.026$). This difference was no longer observed after morphine treatment, which significantly increased sIPSC amplitude in $NL3^{fl/y}$ mice relative to the saline control group for this genotype ($p = 0.018$). Synaptic inhibition onto dopamine neurons is thus enhanced by chronic morphine exposure in $NL3^{fl/y}$;$DAT^{Cre/wt}$ mice, which may explain why they exhibit an attenuation of both psychomotor sensitization (Figure 4) and corresponding fiber photometry signals (Figure 5). There were no significant changes in sIPSC frequency in any group (Figure 6E), consistent with prior evidence that morphine injection does not change basal

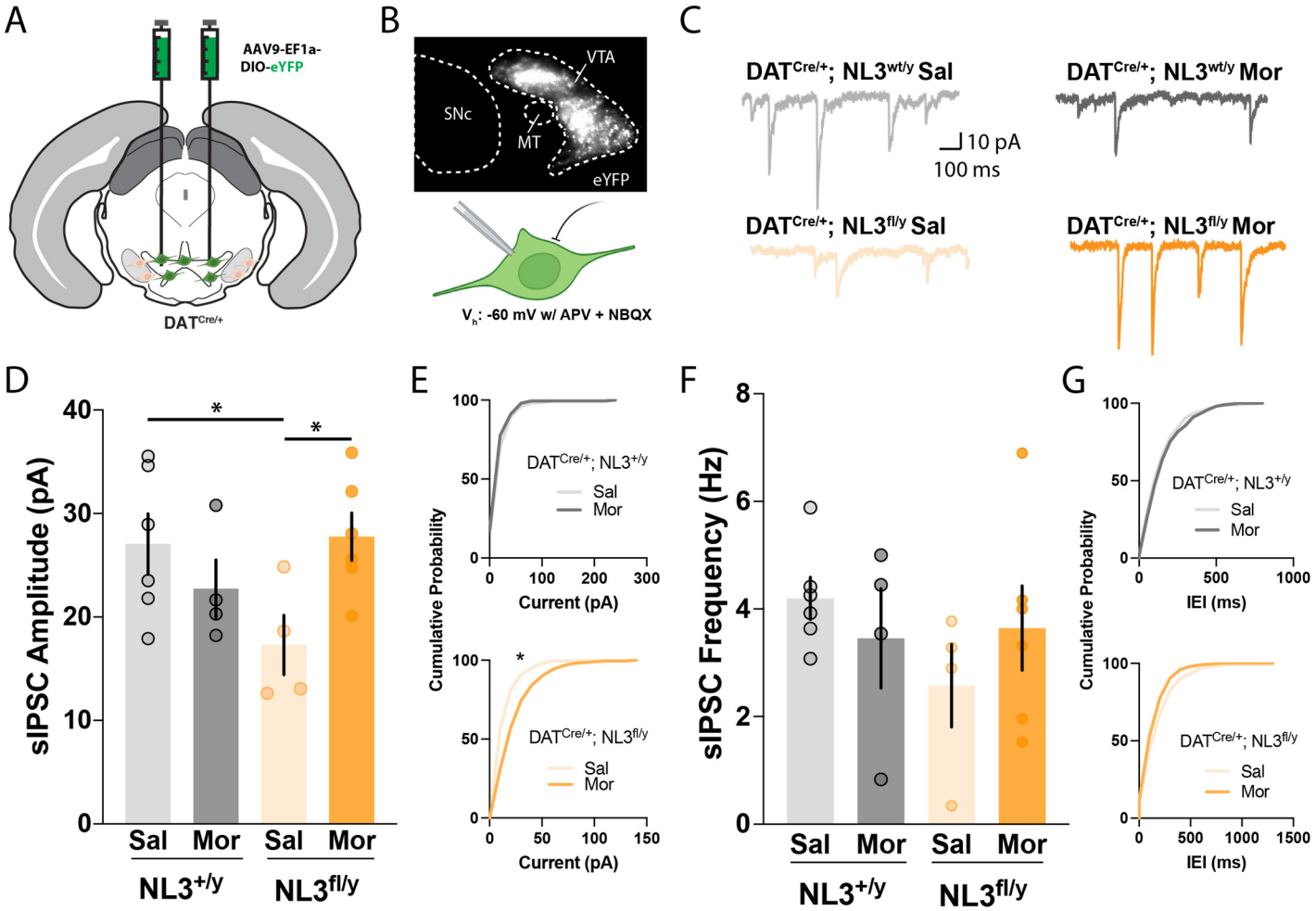


**Figure 6. Synaptic inhibition onto VTA dopamine neurons before and after morphine. (A)** Cartoon showing bilateral stereotaxic injection of AAV9-EF1a-DIO-eYFP virus into the VTA. **(B)** Fluorescent micrograph (top) shows VTA dopamine neurons expressing Cre-dependent YFP in relation to the medial terminal nucleus of the accessory optic tract (MT) and the substantia nigra pars compacta (SNC). Cartoon (bottom) shows recording of spontaneous inhibitory postsynaptic currents (sIPSCs) at a holding potential of -60 mV, in the presence APV and NBQX. **(C)** Example traces from each genotype. **(D)** Average sIPSC amplitude in cells from each group ($NL3^{+/y}$ Sal n=6; $NL3^{+/y}$ Mor n=4; $NL3^{fl/y}$ Sal n=4; $NL3^{fl/y}$ Mor n=6 cells). **(E)** Cumulative probability plots for sIPSC amplitude in $NL3^{+/y}$ (top) and $NL3^{fl/y}$ (bottom). **(F)** Average sIPSC frequency in cells from each group. **(G)** Cumulative probability plots for sIPSC inter-even interval (IEI) in $NL3^{+/y}$ (top) and $NL3^{fl/y}$ (bottom). *p<0.05 comparing groups with Fisher's LSD *post hoc* test **(D)** or the Kolmogorov-Smirnov test **(E)**.

probability of GABA release onto VTA dopamine neurons (Nugent et al., 2007). Together, these data suggest that loss of NL3 expression fundamentally alters the neurobiological adaptations produced by chronic morphine exposure in VTA dopamine neurons, and attenuates the increased dopaminergic sensitivity to morphine normally observed following repeated daily exposure.

## DISCUSSION

Chronic drug exposure causes functional and structural remodeling of synapses in the mesolimbic dopamine system, which could be mediated by synaptic cell adhesion molecules like NL3. Psychomotor sensitization represents a durable enhancement of behavioral sensitivity to morphine that is likely related to synaptic remodeling in the mesolimbic dopamine system. In the absence of NL3, we find that these neuroadaptations appear weakened, leading to a durable attenuation of sensitization. Constitutive NL3 knockout mice exhibit a persistent reduction in the magnitude of psychomotor sensitization caused by intermittent morphine exposure but have a normal psychomotor response to acute morphine. The antinociceptive effect of acute morphine exposure and development of antinociceptive tolerance were also normal in NL3 knockout mice. This rules out global effects on morphine sensitivity due to changes in morphine metabolism or other pharmacokinetic factors, and illustrates specificity in the behavioral impact of NL3 deletion.

We did note that the spatial pattern of locomotor activity, which we refer to as locomotor topography (Mickley et al., 1990), was altered in NL3 knockout mice after both acute and chronic morphine exposure. Mutant mice exhibited a more curvilinear path of travel after morphine injection, bypassing the corners of the chamber and instead traveling through more central areas. While a change in travel through the center of an open field arena is often tied to anxiety-like behavior in rodents, this may not be generally true for C57Bl/6J mice (Thompson et al., 2015), especially following morphine exposure (Hodgson et al., 2010). Instead, the locomotor topography phenotype we observe could be related to the rotational bias previously reported in NL3 knockout mice (Rothwell et al., 2014), although it was only observed after morphine exposure and not after saline injection. A similar pattern has been reported after cocaine (but not saline) injection in mice with a mutation in the serotonin transporter (Simmler et al., 2017). Rotational phenotypes may be exaggerated when elevated levels of extracellular dopamine activate D1 dopamine receptors (Ralph et al., 2001). In the NAc of NL3 knockout mice, D1-MSNs have reduced inhibitory synaptic input (Rothwell et al., 2014), and may thus be primed to drive rotational behavior in the presence of elevated dopamine (Engeln et al., 2021).

Consistent with this hypothesis, conditional knockout of NL3 from D1-MSNs led to a change in locomotor topography after morphine exposure. Previous work suggests this phenotype represents a perseverative pattern of locomotion (Ralph et al., 2001), and could thus reflect an enhancement of repetitive or stereotyped behavior, which has been linked to NL3 expression by D1-MSNs (Rothwell et al., 2014). However, the development of

psychomotor sensitization was not affected by conditional genetic knockout of NL3 from either D1-MSNs or D2-MSNs. In contrast, conditional knockout of NL3 from dopamine neurons led to an attenuation of psychomotor sensitization after chronic morphine exposure, without affecting locomotor topography. Our results thus reveal a clear double-dissociation in the cell types where NL3 expression is normally required for these two behavioral responses. This is an interesting example of a single molecule having dissociable behavioral functions in different cell types and circuits, similar to previous reports with other molecules like Mecp2 (Ito-Ishida et al., 2015).

Both constitutive NL3 knockout and conditional NL3 deletion from dopamine neurons led to a substantial attenuation of psychomotor sensitization, which was evident both during daily morphine injection and following a prolonged drug-free period. This sensitization phenotype was not observed after conditional NL3 deletion from D1-MSNs or D2-MSNs, and thus does not likely involve MSNs in either the NAc or dorsal striatum. Effects on sensitization were robust but not complete, as mice still showed a diminished increase in distance travelled over the course of repeated daily morphine injection. This could be related to compensatory changes that occur in the absence of NL3 expression, including compensation from other members of the neuroligin family, since some phenotypes of neuroligin knockout mice are amplified when multiple family members are deleted (Varoqueaux et al., 2006). Our finding that NL3 is required for full expression of sensitization after chronic morphine treatment implies that this postsynaptic cell-adhesion molecule is an important arbiter of the neuroplasticity induced by repeated morphine.

To manipulate NL3 expression by dopamine neurons, we used a DAT-IRES-Cre mouse line (Backman et al., 2006). It was recently reported that this mouse line exhibits an enhanced locomotor response to novelty, as well as a diminished locomotor response to amphetamine (Chohan et al., 2020). In our initial behavioral studies (Figure 4), these effects of the DAT-IRES-Cre genotype were potentially confounded with NL3 deletion from dopamine neurons. However, any general impact of the DAT-IRES-Cre genotype on locomotion should have been evident during the acute phase of morphine exposure, when the behavior of both genotypes was quite similar. Furthermore, we generated mice for fiber photometry analysis (Figure 5) using a different breeding strategy in which all offspring had the DAT-IRES-Cre genotype. The development of psychomotor sensitization was attenuated in both experiments regardless of breeding strategy, providing further evidence that our results are not confounded by the DAT-IRES-Cre genotype. We used DAT-IRES-Cre mice to selectively target dopamine neurons while avoiding non-dopaminergic cells (Lammel et al., 2015), but it is important to note that

DAT expression is not uniformly high in all dopamine neurons (Morales and Margolis, 2017). Lower DAT expression is observed in mesocortical dopamine neurons (Lammel et al., 2008), so our results may be more closely tied to deletion of NL3 from mesolimbic dopamine neurons.

We directly assessed the function of VTA dopamine neurons using fiber photometry calcium imaging and whole-cell patch-clamp electrophysiology, and found that the impact of chronic morphine administration was either prevented or fundamentally altered in the absence of NL3 expression. After repeated daily morphine injection, the increased calcium signal normally detected in VTA dopamine neurons was not observed after NL3 conditional knockout. This is likely related to an increase in the strength of inhibitory synaptic input onto dopamine neurons that lack NL3 expression following chronic morphine exposure. Surprisingly, that strength of inhibitory synaptic input onto VTA dopamine neurons lacking NL3 was also reduced in saline-treated control mice, relative to the saline control group with normal NL3 expression. However, this reduction of basal synaptic inhibition did not lead to a change in the acute psychomotor response to morphine. This could be due to other cellular or synaptic effects of NL3 deletion, such as increased synaptic incorporation of GluA2-lacking AMPA receptors (Bariselli et al., 2018), which offset the reduction of synaptic inhibition under baseline conditions.

NL3 deletion from VTA dopamine neurons has previously been shown to alter social behavior (Bariselli et al., 2018; Hornberg et al., 2020), and genetic mutations in NL3 have been linked to autism spectrum disorder (ASD) in human patients (Uchigashima et al., 2021). While genetic knockout of NL3 produces forms of synaptic dysfunction that resemble the effects of chronic exposure to drugs of abuse (Carlezon et al., 1997; Bellone and Luscher, 2006; Kim et al., 2011; Koo et al., 2014), we found that NL3 mutant mice were less sensitive to the behavioral impact of chronic morphine exposure. This raises the possibility that drug-evoked forms of synaptic plasticity are occluded by genetic deletion of NL3. Our data also suggest that VTA dopamine neurons exhibit aberrant forms of morphine-evoked synaptic plasticity in the absence of NL3, which may further counteract the effects of addictive drugs. These results are intriguing, given the overlapping circuits implicated in substance use disorders and ASD (Rothwell, 2016), and an evolving understanding of clinical comorbidity between these conditions (Ressel et al., 2020). They suggest NL3 plays a role in both addiction-related synaptic plasticity and other neuropsychiatric conditions, similar to molecules like FMRP (Smith et al., 2014) and MeCP2 (Deng et al., 2014).

## REFERENCES

Backman CM, Malik N, Zhang Y, Shan L, Grinberg A, Hoffer BJ, Westphal H, Tomac AC (2006) Characterization of a mouse strain expressing Cre recombinase from the 3' untranslated region of the dopamine transporter locus. Genesis 44:383-390.

Bariselli S, Hornberg H, Prevost-Solie C, Musardo S, Hatstatt-Burkle L, Scheiffele P, Bellone C (2018) Role of VTA dopamine neurons and neuroligin 3 in sociability traits related to nonfamiliar conspecific interaction. Nature Communications 9.

Bellone C, Luscher C (2006) Cocaine triggered AMPA receptor redistribution is reversed in vivo by mGluR-dependent long-term depression. Nat Neurosci 9:636-641.

Carlezon WA, Jr., Boundy VA, Haile CN, Lane SB, Kalb RG, Neve RL, Nestler EJ (1997) Sensitization to morphine induced by viral-mediated gene transfer. Science 277:812-814.

Chohan MO, Esses S, Haft J, Ahmari SE, Veenstra-VanderWeele J (2020) Altered baseline and amphetamine-mediated behavioral profiles in dopamine transporter Cre (DAT-Ires-Cre) mice compared to tyrosine hydroxylase Cre (TH-Cre) mice. Psychopharmacology (Berl) 237:3553-3568.

Corre J, van Zessen R, Loureiro M, Patriarchi T, Tian L, Pascoli V, Luscher C (2018) Dopamine neurons projecting to medial shell of the nucleus accumbens drive heroin reinforcement. Elife 7.

Deng JV, Wan Y, Wang X, Cohen S, Wetsel WC, Greenberg ME, Kenny PJ, Calakos N, West AE (2014) MeCP2 phosphorylation limits psychostimulant-induced behavioral and neuronal plasticity. J Neurosci 34:4519-4527.

Di Chiara G, Imperato A (1988) Drugs abused by humans preferentially increase synaptic dopamine concentrations in the mesolimbic system of freely moving rats. Proc Natl Acad Sci U S A 85:5274-5278.

Dobi A, Seabold GK, Christensen CH, Bock R, Alvarez VA (2011) Cocaine-Induced Plasticity in the Nucleus Accumbens Is Cell Specific and Develops without Prolonged Withdrawal. Journal of Neuroscience 31:1895-1904.

Docampo E, Ribases M, Gratacos M, Bruguera E, Cabezas C, Sanchez-Mora C, Nieva G, Puente D, Argimon-Pallas JM, Casas M, Rabionet R, Estivill X (2012) Association of neurexin 3 polymorphisms with smoking behavior. Genes Brain Behav 11:704-711.

Doyle MA, Mazei-Robison MS (2021) Opioid-Induced Molecular and Cellular Plasticity of Ventral Tegmental Area Dopamine Neurons. Cold Spring Harb Perspect Med 11.

Durieux PF, Bearzatto B, Guiducci S, Buch T, Waisman A, Zoli M, Schiffmann SN, de Kerchove d'Exaerde A (2009) D2R striatopallidal neurons inhibit both locomotor and drug reward processes. Nat Neurosci 12:393-395.

Engeln M, Song Y, Chandra R, La A, Fox ME, Evans B, Turner MD, Thomas S, Francis TC, Hertzano R, Lobo MK (2021) Individual differences in stereotypy and neuron subtype translatome with TrkB deletion. Mol Psychiatry 26:1846-1859.

Foldy C, Malenka RC, Sudhof TC (2013) Autism-associated neuroligin-3 mutations commonly disrupt tonic endocannabinoid signaling. Neuron 78:498-509.

Georges F, Le Moine C, Aston-Jones G (2006) No effect of morphine on ventral tegmental dopamine neurons during withdrawal. J Neurosci 26:5720-5726.

Gerfen CR, Paletzki R, Heintz N (2013) GENSAT BAC cre-recombinase driver lines to study the functional organization of cerebral cortical and basal ganglia circuits. Neuron 80:1368-1383.

Giza JI, Jung Y, Jeffrey RA, Neugebauer NM, Picciotto MR, Biederer T (2013) The synaptic adhesion molecule SynCAM 1 contributes to cocaine effects on synapse structure and psychostimulant behavior. Neuropsychopharmacology 38:628-638.

Gong S, Doughty M, Harbaugh CR, Cummins A, Hatten ME, Heintz N, Gerfen CR (2007) Targeting Cre recombinase to specific neuron populations with bacterial artificial chromosome constructs. J Neurosci 27:9817-9823.

Graziane NM, Sun S, Wright WJ, Jang D, Liu Z, Huang YH, Nestler EJ, Wang YT, Schluter OM, Dong Y (2016) Opposing mechanisms mediate morphine- and cocaine-induced generation of silent synapses. Nat Neurosci 19:915-925.

Gunaydin LA, Grosenick L, Finkelstein JC, Kauvar IV, Fenno LE, Adhikari A, Lammel S, Mirzabekov JJ, Airan RD, Zalocusky KA, Tye KM, Anikeeva P, Malenka RC, Deisseroth K (2014) Natural neural projection dynamics underlying social behavior. Cell 157:1535-1551.

Hearing M, Graziane N, Dong Y, Thomas MJ (2018) Opioid and Psychostimulant Plasticity: Targeting Overlap in Nucleus Accumbens Glutamate Signaling. Trends Pharmacol Sci 39:276-294.

Hearing MC, Jedynak J, Ebner SR, Ingebretson A, Asp AJ, Fischer RA, Schmidt C, Larson EB, Thomas MJ (2016) Reversal of morphine-induced cell-type-specific synaptic plasticity in the nucleus accumbens shell blocks reinstatement. Proc Natl Acad Sci U S A 113:757-762.

Hishimoto A, Liu QR, Drgon T, Pletnikova O, Walther D, Zhu XG, Troncoso JC, Uhl GR (2007) Neurexin 3 polymorphisms are associated with alcohol dependence and altered expression of specific isoforms. Hum Mol Genet 16:2880-2891.

Hodgson SR, Hofford RS, Buckman SG, Wellman PJ, Eitan S (2010) Morphine-induced stereotyped thigmotaxis could appear as enhanced fear and anxiety in some behavioural tests. J Psychopharmacol 24:875-880.

Hornberg H, Perez-Garci E, Schreiner D, Hatstatt-Burkle L, Magara F, Baudouin S, Matter A, Nacro K, Pecho-Vrieseling E, Scheiffele P (2020) Rescue of oxytocin response and social behaviour in a mouse model of autism. Nature 584:252-256.

Ito-Ishida A, Ure K, Chen H, Swann JW, Zoghbi HY (2015) Loss of MeCP2 in Parvalbumin-and Somatostatin-Expressing Neurons in Mice Leads to Distinct Rett Syndrome-like Phenotypes. Neuron 88:651-658.

Jamain S, Quach H, Betancur C, Rastam M, Colineaux C, Gillberg IC, Soderstrom H, Giros B, Leboyer M, Gillberg C, Bourgeron T, Paris Autism Research International Sibpair S (2003) Mutations of the X-linked genes encoding neuroligins NLGN3 and NLGN4 are associated with autism. Nat Genet 34:27-29.

Johnson SW, North RA (1992) Opioids excite dopamine neurons by hyperpolarization of local interneurons. J Neurosci 12:483-488.

Kim J, Park BH, Lee JH, Park SK, Kim JH (2011) Cell type-specific alterations in the nucleus accumbens by repeated exposures to cocaine. Biol Psychiatry 69:1026-1034.

Koo JW, Lobo MK, Chaudhury D, Labonte B, Friedman A, Heller E, Pena CJ, Han MH, Nestler EJ (2014) Loss of BDNF signaling in D1R-expressing NAc neurons enhances morphine reward by reducing GABA inhibition. Neuropsychopharmacology 39:2646-2653.

Lacey MG, Mercuri NB, North RA (1987) Dopamine acts on D2 receptors to increase potassium conductance in neurones of the rat substantia nigra zona compacta. J Physiol 392:397-416.

Lachman HM, Fann CS, Bartzis M, Evgrafov OV, Rosenthal RN, Nunes EV, Miner C, Santana M, Gaffney J, Riddick A, Hsu CL, Knowles JA (2007) Genomewide suggestive linkage of opioid dependence to chromosome 14q. Hum Mol Genet 16:1327-1334.

Lammel S, Hetzel A, Hackel O, Jones I, Liss B, Roeper J (2008) Unique properties of mesoprefrontal neurons within a dual mesocorticolimbic dopamine system. Neuron 57:760-773.

Lammel S, Steinberg EE, Foldy C, Wall NR, Beier K, Luo L, Malenka RC (2015) Diversity of transgenic mouse models for selective targeting of midbrain dopamine neurons. Neuron 85:429-438.

Lefevre EM, Pisansky MT, Toddes C, Baruffaldi F, Pravetoni M, Tian L, Kono TJY, Rothwell PE (2020) Interruption of continuous opioid exposure exacerbates drug-evoked adaptations in the mesolimbic dopamine system. Neuropsychopharmacology 45:1781-1792.

Lerner TN, Shilyansky C, Davidson TJ, Evans KE, Beier KT, Zalocusky KA, Crow AK, Malenka RC, Luo L, Tomer R, Deisseroth K (2015) Intact-Brain Analyses Reveal Distinct Information Carried by SNc Dopamine Subcircuits. Cell 162:635-647.

Matsui A, Jarvie BC, Robinson BG, Hentges ST, Williams JT (2014) Separate GABA afferents to dopamine neurons mediate acute action of opioids, development of tolerance, and expression of withdrawal. Neuron 82:1346-1356.

Mickley GA, Mulvihill MA, Postler MA (1990) Brain mu and delta opioid receptors mediate different locomotor hyperactivity responses of the C57BL/6J mouse. Psychopharmacology (Berl) 101:332-337.

Morales M, Margolis EB (2017) Ventral tegmental area: cellular heterogeneity, connectivity and behaviour. Nat Rev Neurosci 18:73-85.

Muskiewicz DE, Uhl GR, Hall FS (2018) The Role of Cell Adhesion Molecule Genes Regulating Neuroplasticity in Addiction. Neural Plast 2018:9803764.

Nugent FS, Penick EC, Kauer JA (2007) Opioids block long-term potentiation of inhibitory synapses. Nature 446:1086-1090.

Pascoli V, Turiault M, Luscher C (2011) Reversal of cocaine-evoked synaptic potentiation resets drug-induced adaptive behaviour. Nature 481:71-75.

Pisansky MT, Lefevre EM, Retzlaff CL, Trieu BH, Leipold DW, Rothwell PE (2019) Nucleus Accumbens Fast-Spiking Interneurons Constrain Impulsive Action. Biol Psychiatry 86:836-847.

Radke AK, Rothwell PE, Gewirtz JC (2011) An anatomical basis for opponent process mechanisms of opiate withdrawal. J Neurosci 31:7533-7539.

Ralph RJ, Paulus MP, Fumagalli F, Caron MG, Geyer MA (2001) Prepulse inhibition deficits and perseverative motor patterns in dopamine transporter knock-out mice: differential effects of D1 and D2 receptor antagonists. J Neurosci 21:305-313.

Ressel M, Thompson B, Poulin MH, Normand CL, Fisher MH, Couture G, Iarocci G (2020) Systematic review of risk and protective factors associated with substance use and abuse in individuals with autism spectrum disorders. Autism 24:899-918.

Robinson TE, Berridge KC (1993) The neural basis of drug craving: an incentive-sensitization theory of addiction. Brain Res Brain Res Rev 18:247-291.

Rothwell PE (2016) Autism Spectrum Disorders and Drug Addiction: Common Pathways, Common Molecules, Distinct Disorders? Front Neurosci 10:20.

Rothwell PE, Fuccillo MV, Maxeiner S, Hayton SJ, Gokce O, Lim BK, Fowler SC, Malenka RC, Sudhof TC (2014) Autism-associated neuroligin-3 mutations commonly impair striatal circuits to boost repetitive behaviors. Cell 158:198-212.

Sanders SJ et al. (2011) Multiple recurrent de novo CNVs, including duplications of the 7q11.23 Williams syndrome region, are strongly associated with autism. Neuron 70:863-885.

Schiffmann SN, Vanderhaeghen JJ (1993) Adenosine A2 receptors regulate the gene expression of striatopallidal and striatonigral neurons. J Neurosci 13:1080-1087.

Shuster L, Webster GW, Yu G (1975) Increased running response to morphine in morphine-pretreated mice. J Pharmacol Exp Ther 192:64-67.

Siddiqui TJ, Craig AM (2011) Synaptic organizing complexes. Curr Opin Neurobiol 21:132-143.

Simmler LD, Anacker AMJ, Levin MH, Vaswani NM, Gresch PJ, Nackenoff AG, Anastasio NC, Stutz SJ, Cunningham KA, Wang J, Zhang B, Henry LK, Stewart A, Veenstra-VanderWeele J, Blakely RD (2017) Blockade of the 5-HT transporter contributes to the behavioural, neuronal and molecular effects of cocaine. Br J Pharmacol 174:2716-2738.

Smith LN, Jedynak JP, Fontenot MR, Hale CF, Dietz KC, Taniguchi M, Thomas FS, Zirlin BC, Birnbaum SG, Huber KM, Thomas MJ, Cowan CW (2014) Fragile X mental retardation protein regulates synaptic and behavioral plasticity to repeated cocaine administration. Neuron 82:645-658.

Sudhof TC (2017) Synaptic Neurexin Complexes: A Molecular Code for the Logic of Neural Circuits. Cell 171:745-769.

Sun L, Hu L, Li Y, Cui C (2014) Mesoaccumbens dopamine signaling alteration underlies behavioral transition from tolerance to sensitization to morphine rewarding properties during morphine withdrawal. Brain Struct Funct 219:1755-1771.

Tabuchi K, Blundell J, Etherton MR, Hammer RE, Liu X, Powell CM, Sudhof TC (2007) A neuroligin-3 mutation implicated in autism increases inhibitory synaptic transmission in mice. Science 318:71-76.

Thompson T, Grabowski-Boase L, Tarantino LM (2015) Prototypical anxiolytics do not reduce anxiety-like behavior in the open field in C57BL/6J mice. Pharmacol Biochem Behav 133:7-17.

Toddes C, Lefevre EM, Brandner DD, Zugschwert L, Rothwell PE (2021) mu-Opioid Receptor (Oprm1) Copy Number Influences Nucleus Accumbens Microcircuitry and Reciprocal Social Behaviors. J Neurosci 41:7965-7977.

Uchigashima M, Cheung A, Futai K (2021) Neuroligin-3: A Circuit-Specific Synapse Organizer That Shapes Normal Function and Autism Spectrum Disorder-Associated Dysfunction. Front Mol Neurosci 14:749164.

Varoqueaux F, Aramuni G, Rawson RL, Mohrmann R, Missler M, Gottmann K, Zhang W, Sudhof TC, Brose N (2006) Neuroligins determine synapse maturation and function. Neuron 51:741-754.

Vezina P, Leyton M (2009) Conditioned cues and the expression of stimulant sensitization in animals and humans. Neuropharmacology 56 Suppl 1:160-168.

Vezina P, Kalivas PW, Stewart J (1987) Sensitization occurs to the locomotor effects of morphine and the specific mu opioid receptor agonist, DAGO, administered repeatedly to the ventral tegmental area but not to the nucleus accumbens. Brain Res 417:51-58.

Zhang Y et al. (2021) Fast and sensitive GCaMP calcium indicators for imaging neural populations. bioRxiv:2021.2011.2008.467793.